A comparison of two methods for natural landmark classification with Biosonar

Maosen Wang, Rolf Müller and Andreas Zell

WSI-2006-05

Maosen Wang and Andreas Zell
Wilhelm-Schickard-Institute für Informatik
University of Tübingen
Sand 1
D-72076 Tübingen
Germany
Email:{wangm,zell}@informatik.uni-tuebingen.de

Telefon: (+49)7071 29 77175
Telefax: (+49)7071 29 5091

Rolf Müller
Maersk McKinney Moller Institute for Production Technology
Unversity of Southern Denmark
Campusvej 55
DK-5230 Odense M
Denmark
Email: rolfm@mip.sdu.dk

Telefon: (+45)65 50 3655
Telefax: (+45)66 15 7697

© Wilhelm-Schickard-Institute für Informatik, 2006
ISSN 0946-3852

ISSN 0946-3852

A comparison of two methods for natural landmark classification with Biosonar

Maosen Wang, Rolf Müller, and Andreas Zell

Computer Science Dept.,
University of Tübingen,
Sand 1, 72076 Tübingen, Germany,
{wangm,zell}@informatik.uni-tuebingen.de

Abstract. Most current sonar systems for mobile robots only yield time of flight distance information produced by measuring the time of a single sonar pulse. However, sonar systems of animals like sonar bats are much more sophisticated, allowing to recognize not only the shape, but also the type of landmark trees that they use during their nocturnal flights. In this paper we compare two methods for natural landmark classification by a biomimetic sonar consisting of one sender (mouth) and two receivers (ears). Our research aims to improve the navigation capabilities of mobile robots in natural and man-made environments, where economical and robust feature extrcation of potential landmarks such as trees is a key problem. We try to classify different species of trees from random orientations. Two methods utilized are intricate structure feature based and general structure feature based natural landmark classification. After a comparation of those two method's advantages and disadvantages, we forwarded a two-step Biosonar classification strategy for outdoor navigation of mobile robots. Experimental results indicate that a mobile robot with such a Biosonar system can achieve the ability to classify natural landmarks like trees only based on sonar.

1 Introduction

The problem of recognizing landmarks in natural environments is important for the navigation of mobile outdoor robots. Besides camera, laser scanner, radar and IR sensors, in-air sonar can also yield useful information for landmark classification. Leonard and Durrant-whyte used the feature of Region of Constant Depth for navigation[**?**]. Kimoto and Yuta detected hedge with standard deviation of range readings[**?**]. Mckerrow extacted features both for indoor and outdoor landmark classification[**?**][9]. L.Kleeman achieved accurate measurment and classification of three target types(plane, corner and edge)[**?**]. Roman Kuc tried to recognize penny coin using binaural information of a bioninetic sonar system[**?**]. Rolf Mueller made classification of 4 trees with the feature of Distant Interspike Intervals[10][1] .

In this paper we try to extend previous research into the practical application by comparing two natural landmark classification methods, which are respectively based on intricate structure features and general structure features.

To be a suitable landmark, the target should meet several requirements [3]: frequent occurrence, slow changes and easy classification. Plants can meet those requirements only if the third requirement is met. We study this problem with artificial trees, because they

[1] Biosonar laboratory of Prof. Dr. Schnitzler, Tuebingen University

are typical multi-facet plants that have rich overall and detailed construction differences, such as

– scale, form, density and degree of symmetry;
– leaves' direction, flatness and size;
– for sparse trees, the exposed trunks also play a significant role in reflected signals.

The task of natural landmark classification has two sides. It needs both enough feature difference between different targets and sufficient feature similarity among samples of similar targets from different orientations and ranges. This demands the extraction of robust features from the Biosonar signals, which look rather similar to white noise to the naked eye.

The organization of this paper is the following: section 2 describes our echo model, section 3 introduces the Biosonar system used here. Section 4 presents a classification method with intricate structure features, section 5 a classification with general structure features. A comparison of those two methods is given in section 6, while experimental results are listed in section 7.

2 Echo model

How much information can we extract from Biosonar? Let us take a look at our echo model. In figure 1 there are signals of two types of leaves. One is a piece of a $6 \times 11cm$ schefflera leaf, the other is a cluster of five $1.2 \times 6.5cm$ bamboo leaves.

Their respective signals after band pass filtering ($f_c = 50kHz$) show: The large leaf is not flat, its different parts of surfaces can reflect in the way of several leaves of various sizes in different distances. A cluster of leaves in certain distribution can reflect together like a big leaf. We define A_i, the changing reflection from one leaf, as the result of following factors:

$$A_i(t) = f_i(d_i, \theta_i, \varphi_i, p_i, s_i(t)) \tag{1}$$

where f_i is the reflection function of a leaf with certain form and size, d_i the two-way distance from leaf to Biosonar (D1 in figure 2), θ_i the leaf's horizontal orientation angle to the Biosonar, φ_i the leaf's vertical orientation angle to Biosonar, p_i the space posture of the leaf itself (3D angles), $s_i(t)$ the chirp signal sent for probing. It is much more complex than the following reflection model, valid for plane waves and infinite planar surfaces [7]. And other models, that deal with single geometrical features such as edge, corner, plane [6] and radius of curvature [1], can not represent echo from the irregular curving foliage surface.

$$\alpha(\omega) = 1 - |R(j\omega)|^2 \tag{2}$$

$$R(j\omega) = \frac{Z(j\omega) - 1}{Z(j\omega) + 1} \tag{3}$$

where $\alpha(\omega)$ is the absorption coefficient, $R(j\omega)$ the reflection coefficient and $Z(j\omega)$ the normalized impedance.

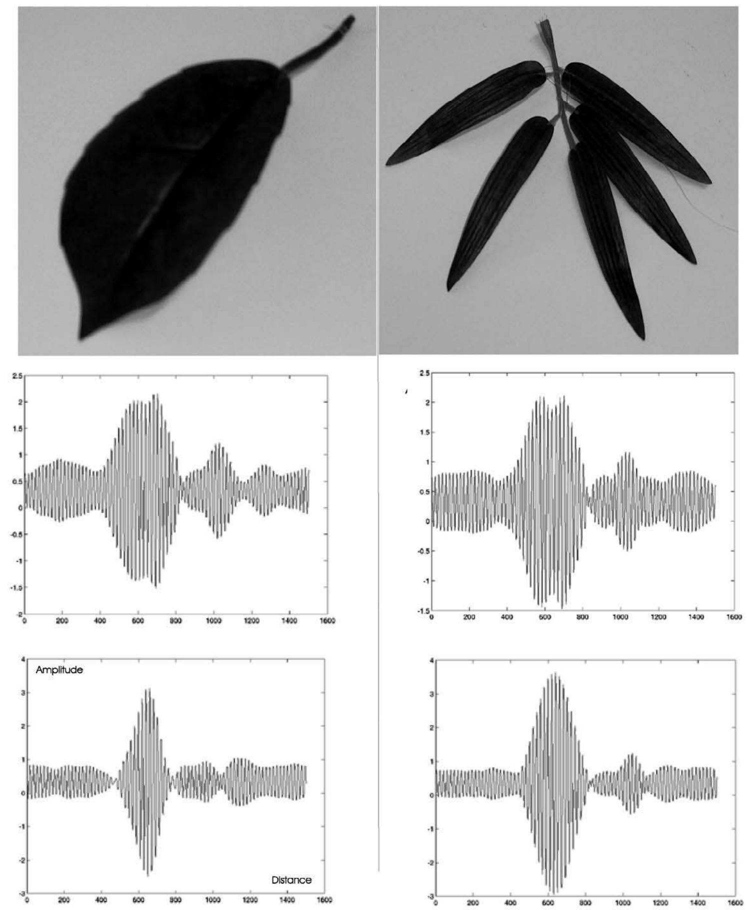

Fig. 1. Leaves scanned by sonar from 2 directions

The information in each resulting echo $A(t)$ of a tree looks like a white noise signal except for TOF information. One may think, when the chirp is a very short pulse, $A(t)$ denotes the reflection magnitude from a series of elliptical target surfaces in 3D space, where $D_i = d_{i1} + d_{i2} = v(t_{i1} + t_{i2})$. In fact the amplitude of chirp always suffers from serious lateral and axial superimposition, which is unpredictably constructive or destructive due to the lacking of precise geometrical model of all leaves and their spatial orientation and position. So, each $A(t)$ is only a unpredictable superimposition of reflections from some reflecting units of some 'visible' leaves, it's information about a tree is incomplete and distorted.

$$A(t) = F(\Theta_1 A_1(t), \Theta_2 A_2(t), ...\Theta_i A_i(t), ...) \tag{4}$$

where F is the superposition function, $i \in 1, 2, ...N$ is the leaf number, $\Theta_i \in [0, 1]$ denotes the degree of exposure of individual leaf i.

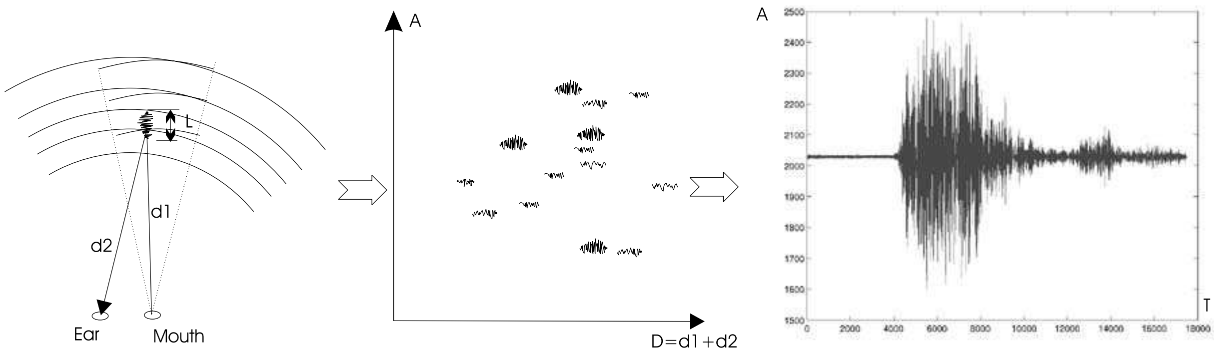

Fig. 2. Superposition from individual leaf reflections to echo of the tree

When we further consider factors of Biosonar system noise and environment variance generated by wind, temperature and humidity, there are in fact no identical $A(t)$ at all. Experimental results from the same test arrangement in 0.05s intervals in the laboratory verified this. As a result, the problem of multi-facet target classification is mainly a task to find feature likelihood between samples and templates.

From the understanding of echo and this model $A(t)$, we can see that differences in trees can not always lead to very different Biosonar observation. The echoes from trees are profoundly stochastic [11], they are individually incomplete and unpredictably distorted. The kernel problem is how we can utilize those observations wisely although they can never match images of light. Two methods introduced in this paper extract features that represent intricate structure and general structure differences respectively. A k-nearest neighbour classification algorithm is used to make the classification decision.

3 Biosonar System

We used a Biosonar head which consists of 3 Polaroid sensors in a triangular layout , which simulates the layout of a bat's mouth and ears[12]: two Polaroid 600 sensors spaced 12.5cm apart as ears, a Polaroid 7000 sensor as mouth in the middle between the two ears but 2.5cm lower (figure 3). With two turning ears, which have two degrees of freedom each, we can not only obtain a measurement of the target's distance and bearing to the robot by calculating time of flight (TOF), but also enhance the signal to noise rate (SNR), or even get pairs of crossed echoes that record more information of targets like a cubic view.

The hardware of our Biosonar system consists of an Intel Pentium 4 computer, a National Instruments NI6110 analog I/O card, a Mini SSC$\prod$ serial servo controller, a BNC2110 connector, a NiMH charger box and this Biosonar head (figure 4). The sampling speed of the NI6110 card is 5Mhz, we utilize 1Mhz in our research. The NiMH charger box provides the sensors with a 150V power supply.

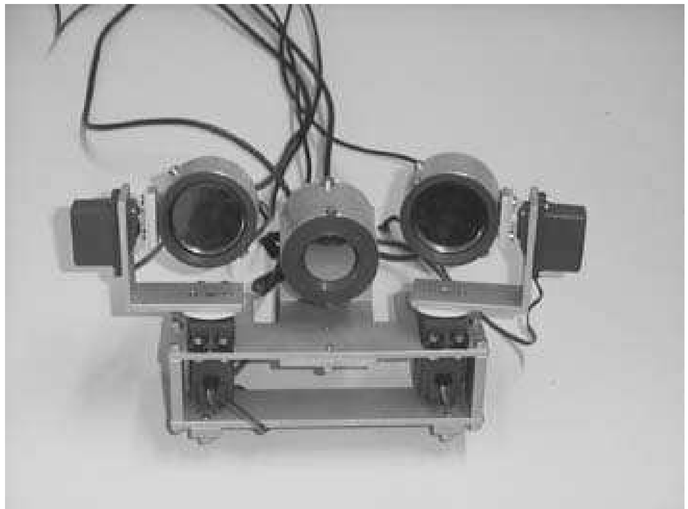

Fig. 3. Biosonar head

The software consists of four layers in RedHat Linux7.3, an additional free driver software is crucial for the card to achieve 1Mhz analog input sampling speed (figure 5).

4 Intricate structure features

When bats hover above their prey, they emit calls during all stages [13]. The harmonic pattern of the calls differs greatly between aimless searching and target detecting stages. They emit long chirps (4ms) with more energy, which are suitable for travelling long distances when they search targets, but use short and higher frequency chirps to probe a near target that may be a potential prey. They also lower chirp's intensity as they approach a large target, in order to maintain the echo intensity within a suitable range for auditory

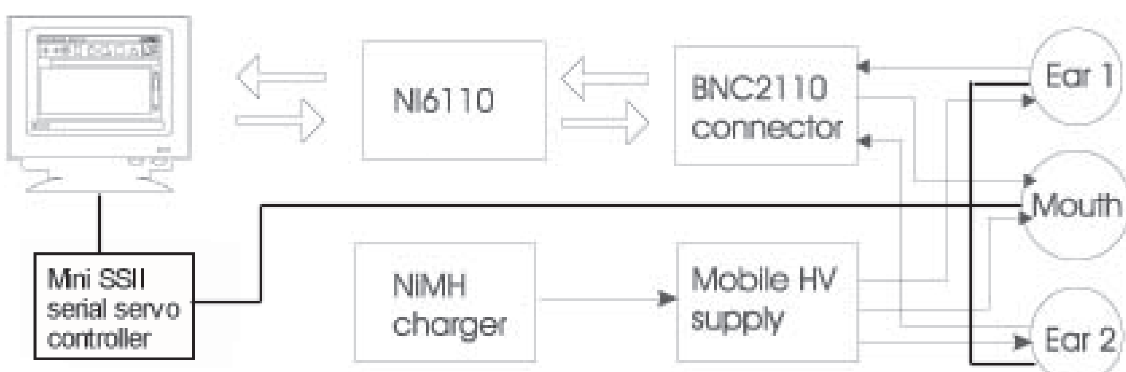

Fig. 4. Biosonar system

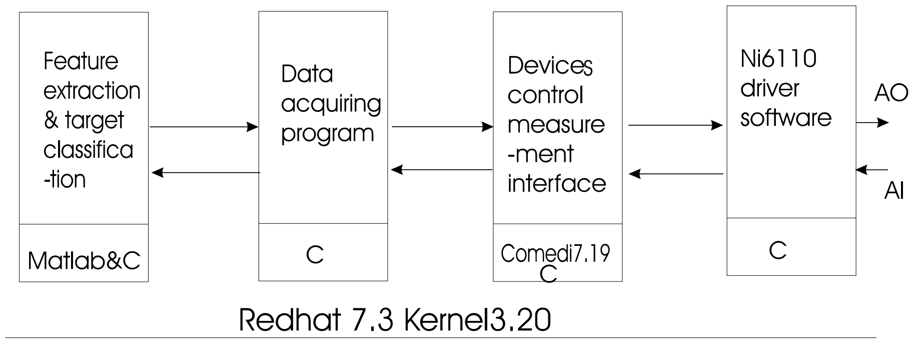

Fig. 5. Software structure

processing [4]. Inspired by those phenomena and based on our $A(t)$ echo model (section 1), we utilized the chirp as short as the signal to noise rate (SNR) allowed and adjusted the range of analog I/O card dynamically to achieve suitable amplitude resolution. With the hope for enhanced axial resolution, we tried 0.256ms, 0.512ms and 1.024ms chirps, which were linearly frequency modulated (figure 6).

The classification results with 2 intricate structure features verified this idea. Two features, distant interspike interval [10] and low frequency variance, come respectively from the temporal and spectral domain. They reflect intricate structure differences of trees.

4.1 Distant interspike interval

This approach was formerly introduced by our former cooperation partner [10]. There, the classification was carried out with 3ms chirps from 3D space in a limited orientation range with $84,800$ echoes for the classification between 4 plants. The method proposed here attempts the classification with chirps from the full 2π range 2D plane with shorter and fewer chirps (figure 6), aiming at practical usage by mobile robot navigation. It needs 720 echoes' feature template for each plant and 20 to 80 echoes' probing by classification. Furthermore, the kernel algorithm of the sequential probability ratio test (SPRT) [2] is different.

The key idea of the distant interspike interval feature is to study the tiny reflection decreases in the acoustic density profile of echo. The acoustic density profile models the structure of plant foliage [9]. According to our model $A(t)$, the decreases, which are longer than the carrier wave's length λ, shall statistically represent a tree's intricate structure distributed in successive elliptical surfaces e_i (figure 2 left).

The extraction of those long duration echoes is described in figure (8). First a gammatone band pass filter is used to get an array of filtered waves whose surface simulates the motion of the basilar membrane as a function of time. It provides a reasonable trade-off between accuracy in simulating basilar membrane motion and computational load. The impulse response of the gammatone is [15]:

$$g_t(t) = at^{n-1} \exp(-2\pi bERB(f_c)t) \cos(2\pi f_c t + \phi) \tag{5}$$

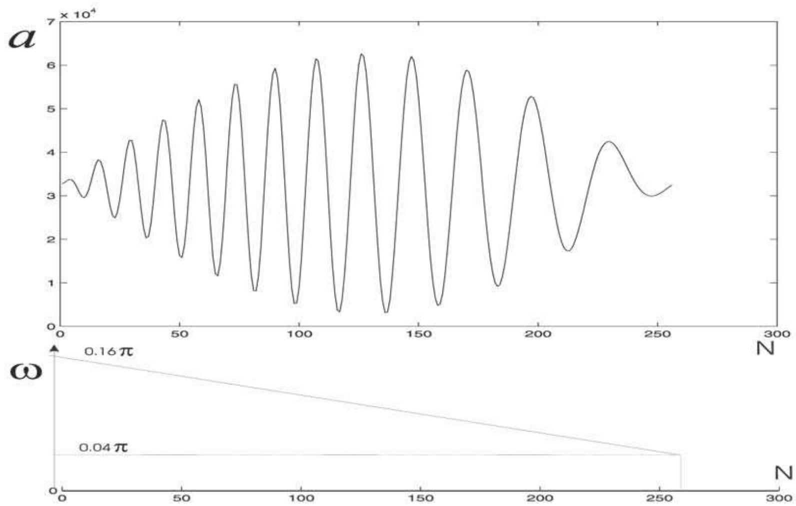

Fig. 6. 256 points linearly frequency modulated chirp (256us duration, 50kHz central frequency)

where time $t > 0$, a is the amplitude, n and b are parameters defining the envelope of the gamma distribution, and f_c is the centre frequency. ϕ is the initial phase. $ERB(f_c)$ is the equivalent rectangular bandwidth of the filter(ERB), and at moderate levels $ERB(f_c) = 24.7 + 0.108 f_c$ in Hz [5]. The symmetrical output array is half wave rectified and low pass filtered to get the acoustic density profile of echo. The moving average filter used here is a 50 point filter:

$$\mathrm{y[i]} = \frac{1}{50}\sum_{j=0}^{49} x[i+j-25] \tag{6}$$

Then the increasing slope of the resulting signal(see figure 2), which is between the edge of the first noise threshold crossing and the maximum amplitude position, is horizontally and evenly divided by 129 amplitude stages. The horizontal width of every small part of slope is D_{ij}. From series of echoes, a metric (D_{ij}) is achieved.

$$(D_{ij}) = \begin{pmatrix} D_{11} & D_{12} \dots & D_{1n} \\ D_{21} & \dots & \dots & \dots \\ \dots & \dots & \dots & \dots \\ D_{m1} & \dots & \dots & D_{mn} \end{pmatrix} \tag{7}$$

where m denotes the total echo number in a sample group , n is the total number amplitude range by every echo. $j \in n$ denotes the amplitude by every D_{ij}. In this way, the amplitude normalization is also achieved. With 1Mhz digital sampling rate and 50kHz centre frequency band pass filter, the long decreases are extracted with threshold $D_{ij} > 0.03ms$, which is 50% longer than the $0.02ms$ wave length of $50Khz$ (figure 7). Those decreases are named as distant interspike intervals (DIIS).

$$(D_{ij}) \overset{|D_{ij}|>=0.03}{\rightarrow} (DII) \rightarrow (\overline{\Delta_i}, \overline{a_i}, \overline{p_i}, N_i) \tag{8}$$

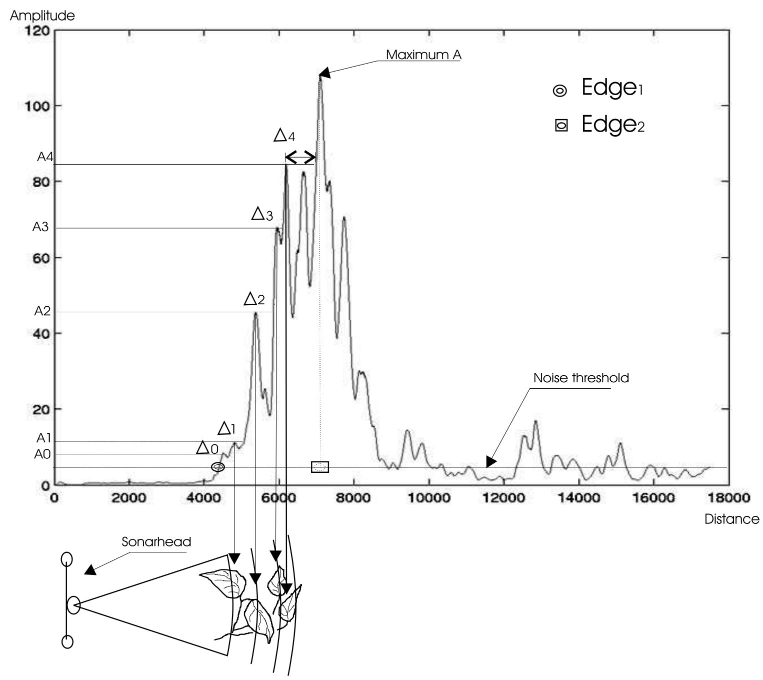

Fig. 7. Extaction of distant interspike intervals

Four parameters of DII are recorded from each echo:$(\overline{\Delta_i}, \overline{a_i}, \overline{p_i}, N_i)$ where $\overline{\Delta_i}$ is the mean duration time of a DII in echo i, $\overline{a_i}$ is the mean amplitude of a DII in echo i, $\overline{p_i}$ is the DII horizontal position to the first position that signal goes above noise threshold$(edge(1))$, N_i is the total number of DII in echo i.

From repeating echoes generated by natural landmarks we calculate the probability density distribution (PDF) function of those parameters and perform a sequential procedure for multihypothesis test. Let f_j be the PDF result of the upper parameters from templates, target's PDF be f and H_j be the hypothesis that $f \approx f_i$ for $j = 0, 1, ..., M-1$, where M is the total number of hypotheses. The π_j denotes the prior probability of H_j for N tests. There are m echoes for each H_j. The posterior probability p_m^j is:

$$p_m^j = P\{f \approx f_j | f_1, f_2, ..., f_m\} = \frac{\pi_j \prod_{i=1}^{m} f_j(x_i)}{\sum_{k=0}^{M-1} \pi_k (\prod_{i=1}^{m} f_j(x_i))} \tag{9}$$

The original algorithm of M-ary sequential probability ratio test(MSPRT) [2] is: N is the first $m \geq 1$ such that $p_m^j > (1/(1+A_k))$ for at least one k

$$H = H_n \tag{10}$$

$$n = \arg\max_j p_N^j \tag{11}$$

When testing many samples with similar likelihood, $p_m^j > (1/(1+A_k))$ is often reached by more than one j hypothesis at same time. When we use maximum p_m^j for supporting decision, there are also many equal p_m^j by maximum number of tests. So we add three calculation in this algorithm. Those calculations add the choices for selecting the highest $p_m^j > (1/(1+A_k))$ or p_m^j in one round of test, assigning divided possibility to all potential choices with the same $p_m^j > (1/(1+A_k))$ or p_m^j, avoiding 0 priority problem in no hypothesis test round.

In figure(8), the k-nearest neighbour classification algorithm uses 8 rows multivariate hypothesis metric to vote for classification. Seven rows are calculated from the PDF and joint PDF likelihood of $(\overline{\Delta}_i, \overline{a_i}, N_i)$. Here we temporarily do not use $\overline{p_i}$, while its efficiency needs further test. The $8th$ row is from the following feature of low frequency variance.

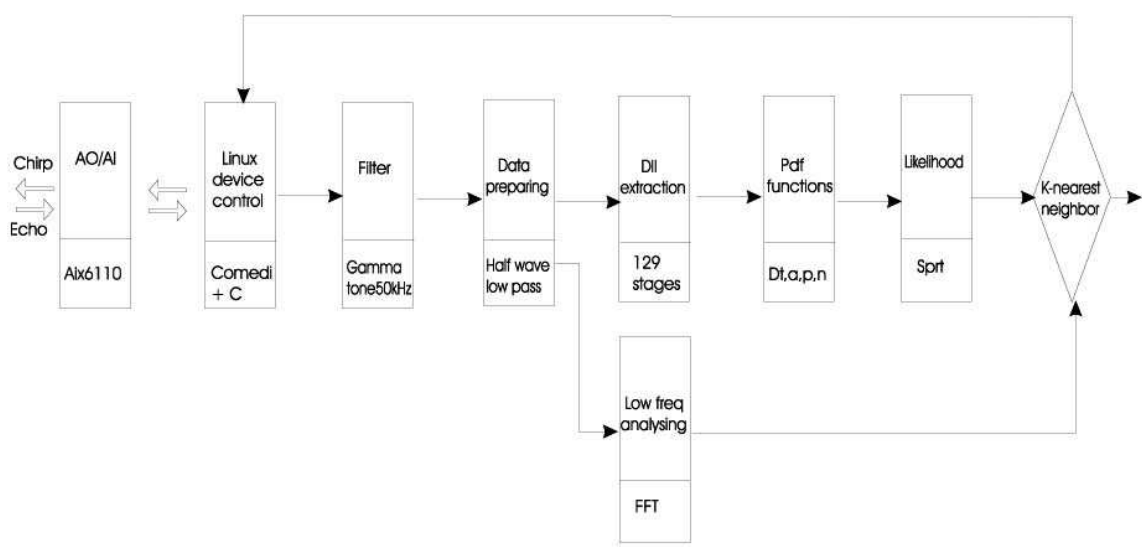

Fig. 8. The process of the first method

The sampling strategy is also decisive for the classification performance. The brittleness of the signal $A(t)$ leads to salient DIIs, which in turn demand a large number of data for statistical analysis. But the time and computing power of a moving mobile robot is limited. This conflict is solved through biological sampling strategies. On one hand, bats do not need to recognize anything they meet; on the other hand, bats obtain just enough information to be characteristic of the targets of their interest. We use a two step classification strategy (section 6) and store DII feature values from 20 to 80 echoes according local asymmetry in every 10 degree range.

The advantages of DII features are that they reflect intricate structure information of a target, and are relatively independent of the target's size, if the ensonified area always covers the main sonar wave lobe. Two disadvantages are (1) Classification rate depends heavily on the numbers of echoes; (2)DIIS from 3D echoes have richer target information than DIIs from 2D. They make this algorithm still not very practical by 2D mobile robot navigation, where quick decision is of of significant worth.

4.2 Low frequency variance

Another feature to study intricate structure information of plants is to analyse average low frequency variance in echoes. We can discriminate the an object from spectrum of the echoes ([14]). From the analysis of $A(t)$ (section 1), we know that each echo from a multi-facet target is the superimposed result of many A_i from individual leaves. Those A_i correspond directly to the leaves' size and positions in a small bearing range, which is characteristic of a tree and leads to the low frequency periodicity variance after leaves' superposition (figure 2). It is just another method to study FM Sonar Image [8] of target. The process of extracting low frequency variance is described in figure 8. A normalization is performed before band pass filtering or after low pass filtering. Then we use Fast Fourier Transform(FFT) to reveal periodicities in the echo as well as the relative strengths of any low frequency components. We find that the schefflera tree has larger spectral response around $1KHz$, which perhaps correspond to its $17cm$ long leaves or 3 sparsely distributed branches. The ficus tree has lowest spectral response, which may correspond to its $3-4cm$ and evenly distributed leaves. The result is reversed around $20kHz$, where the Schefflera tree has lowest response and the ficus has the largest. The bamboos, which have few narrow leaves($0.8cm$) and consist mainly of $1.2cm$ diameter long trunks, has always the medium response after normalization. But without normalization bamboos have always the lowest spectral response. We extracted the mean spectral response values of different plants in various low frequency ranges, and calculate their distance for the $8th$ row value in the above k-nearest neighbour classification.

The advantage of this feature is to classify targets with similar form, size and unbiased space distribution. But it is statistical result and depends on distance obviously. The far big leaves' low frequency variance is similar to small leaves' in the near when the compensation problem mentioned above is not resolved. So we don't use it alone at present.

The k-nearest neighbour algorithm based on 8 parameters from the above 2 feature groups was tested with 3 artificial plants. With 36 template knowledge each, the $360°$ bearing range classification probabilities of ficus, bamboos and schefflera with one glimpse of 20 echoes' sampling are respectively 84%, 72% and 51%. The relative lower classification rate of schefflera tree is obviously due to its relative serious asymmetry, which reflect the first disadvantage of this algorithm.

Num	Name	formula	Denotation
1	Sum-area	$S_i = \sum_{k=edage1}^{edage2} A_{ik}$	effective refelction area
2	max amplitude	$X^i_{\max} = \max_i (A_i(j) / \sum_{j=1}^{n} A_i(j))$	the largest reflecting ability
3	mean amplitude	$X^i_{mean} = \sum_{j=1}^{n} A_i(j)/n$	average reflection ability
4	crest factor	$X^i_c = X^i_{\max} \,/\, X^i_{rms}$	impulsiveness of echo
5	wave form distance	$d_{ij} = \sum_{k=1}^{n} (\overline{A}_i(k) - \overline{A}_j(k))$ $\overline{A}_i = \sum_{l=1}^{m} A_i(l)/m$	envelope matching degree
6	Depth	$D_i = \overline{(edge(2) - edge(1))}$	scale of target

5 General structure features

Another method we utilized is to make classification with 9 time domain features, which represent overall structure information in the echo.

At first we utilize following 6 features extracted from groups of echoes.

Those features' performance varies under different circumstances. In order to reduce their dependence to distance and keep the relative amplitude difference, we perform normalization before calculating them (figure 9).

For every feature f_i a 2D array $f_i(\theta, d)$ is sampled and stored as template. θ is the horizontal orientation, d the distance between Biosonar head and target and i the feature number. Then we use a Kolmogorov-Smirnov test to calculate the similarities respectively before the voting of K-nearest learning.

$$K^2 = \sum_{i=1}^{k} \frac{(EXP_i - OBS_i)^2}{EXP_i} \tag{12}$$

A training algorithm to adaptively give different weights to those features under different circumstances is needed here. In experiments with identical weights of the 6 features, the classification rate of this method for the 3 trees investigated is 87%.

Then we utilize 3 features extracted from sequential echo groups, while we believe also that the sequences of echoes will provide more information to the flying bat [16]. And this sequence is decided by the relative sampling movement between Biosonar and target, here we have used simple turning movement to simulate the hovering of bat. The 3 features are directly from the filtered amplitude envelope:

- local maximum(peaks) position in sequence;
- signature of upper 6 features in sequence;
- image of amplitude envelope in sequence.

In simple echo those features are fast useless for classification due to the character of airborne reflection (section 2. But after adding the new dimension of movement sequence and using 2D matching algorithm, the classification rate rises dramatically(over 95%).

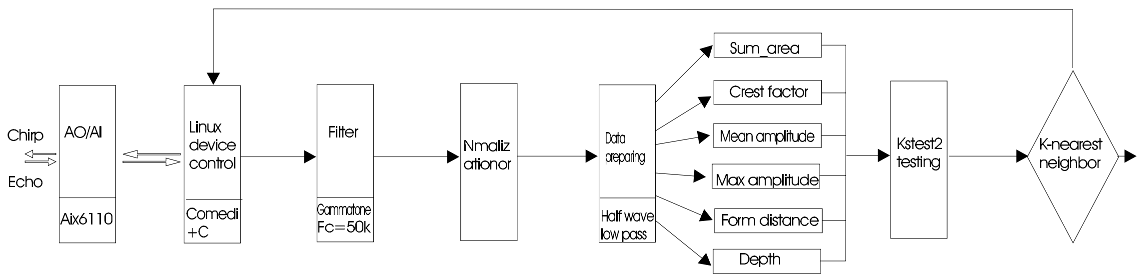

Fig. 9. Extraction of 6 general structure features

6 Comparison of the two methods

The method in section 3 utilizes 2 features that reflect intricate structure information of multi-facet targets in the time and spectral domain. They look into the tiny fluctuation in target reflection. But as holds for many combined probability density functions, their calculation time is much longer than the one of the second method, and the first method also needs rich echoes for precise classification [10], especially by asymmetrical targets, which makes this method not so ideal to perform classification in real time navigation.

The second method in section 4 can quickly make classifications. When used alone, some simple features' positive evaluation of a target may be doubtful, but the negative classification result is trustworthy. When used in combination, especially in sequential probing, they can also achieve high classification rate. We therefore conceive a two step classification strategy for mobile robots. In natural environments, most of the targets hit by a mobile robot's Biosonar are not so important that they must be precisely classified. So during most of the navigation time the mobile robot uses only few simple features from the second method to remove objects from attention. Only when potential landmark objects appear, the first method or the sequential probing of the second method are carried out to make classification certain. This strategy can reduce calculation effort.

7 Experimental results

All tests in this section were performed with 3 artificial trees with similar height of 1.7m (figure 10). A 256 points linearly frequency modulated chirp under 1Mhz sampling rate was used in the following tests. Every glimpse's sampling includes 20 to 80 echoes that collect data in 10 degree bearing range of the target, and every stored feature template is extracted from one glimpse.

7.1 Test 1: Intricate structure features

After we have first verified the classification ability [10] of DIIs with 1024 echoes from limited orientation range(10 degree) in 2D plane, where classification can easily reach

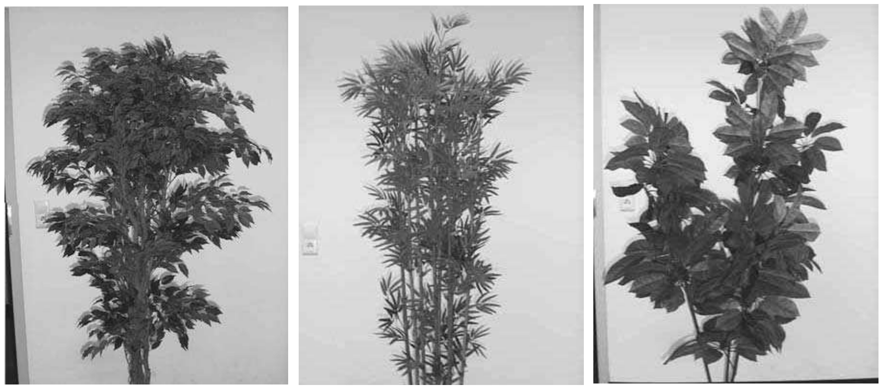

Fig. 10. Three plants: ficus,bamboos and Schefflera

above 95% with a few orientation ranges. We try to make it applicable by mobile robot navigation: classification from all possible orientations and with fewer sampling echoes. We define that a glimpse here means 20 echoes from every 10 degree orientation. The classification rate of one glimpse varies with the acquired knowledge of the target(number of stored glimpses for each target). In the first test, one glimpse's classification rate is tested with 1,3,6 12,24,36 stored template glimpses, which is evenly sampled from $360°$ bearing range. The results from more than a thousand tests are listed in figure (11). We find that:

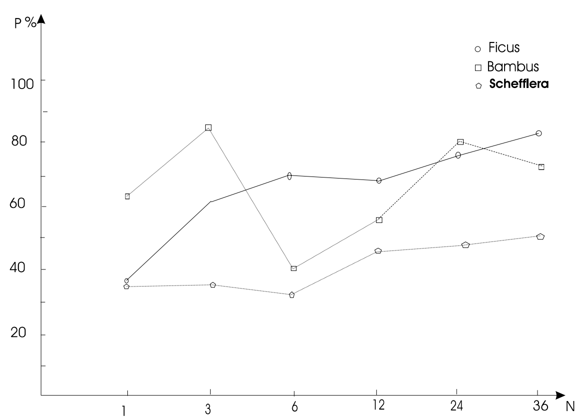

Fig. 11. Classification rate from comparing one glimpse with different number of stored glimpses by first method

- The classification rate increases slowly with the increasing numbers of templates, which are evenly distributed in $360°$ bearing range. The temporary decreases in increasing tendencies are the result of likelihood competition of other classes. Since the number of templates for each plant is always the same, the probability of other classes' template with similar feature increases together with increasing template's number.

- In theory this method can precisely make statistic classification of multi-facet targets when there are enough many echoes from different orientations. But a asymmetrical target like schefflera here demands more echoes from the same bearing range.
- The DII features obtained from local views of the trees are mostly leaf based. They are very salient, because one leaf, which is hit by the main sonar lobe and whose normal axis is close to the Biosonar sound axis, can easily change the D_{ij} data from an echo. When DIIs come from clusters or branches instead of individual leafs and the whole plant is covered by the sonar cone, they can be more stable.
- With one glimpse, plants of different size can be classified with 15% error probability , but lower by similar scale .
- The P parameter from the DII feature has more stable performance when we collect no less than 80 echoes per template for classification. The error probability is 81% with 80 echoes' template vs. 43% with 20 echoes' template. This is the most promising parameter of these DII features.

7.2 Test 2: General structure features

In this test, we first ignored the probing sequence and used 6 features to classify with different numbers of intricate general feature templates (figure 12):

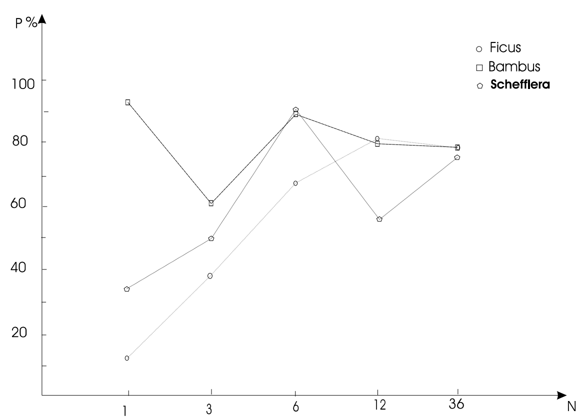

Fig. 12. Classification rate from comparing one glimpse with different number of stored glimpses by second method

From result of this test we find:

- One feature alone can not precisely describe a multi-facet target like a tree. A classification of certain targets needs the use of different features.
- The 6 features used in this method are extracted after normalization. We shall use $A(t)/\sum A(t)$ instead of $A(t)/max(A(t))$ in order to make the maximum amplitude comparable between targets.
- This method's classification rate may decrease when there is a large potential choice of targets, but it is powerful to take most of calculation burden for classification.

- Among the 6 features the wave form distance worked best and can even to some degree determine the relative bearing angle of Biosonar to target.

Then we used the other 3 features(local maximum position, combined signature of upper 6 features and envelope image in sequence) filtered from observation by turning movement. The sampling density is $20echoes/10degree$(figure 13). The classification

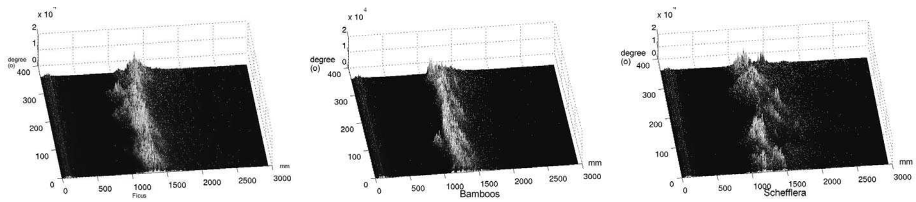

Fig. 13. ficus,bamboos and Schefflera amplitude image one round turning

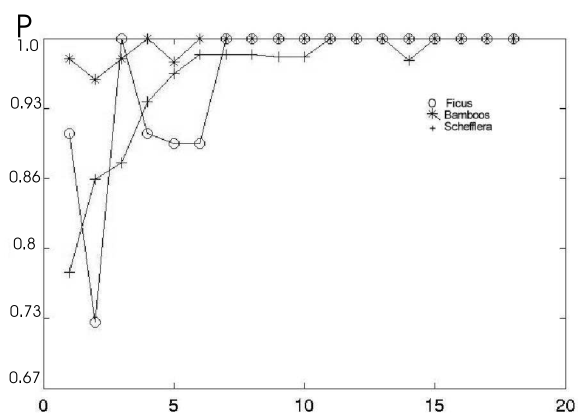

Fig. 14. Classification rate of sequential echoes from different orientation ranges of observation

rate by using different numbers of echoes is list in (figure 14), where horizontal axis(1 to 18) denotes probing range(10 to 180 degrees). From result of this test we find:

- The sequences of echoes' variation providing useful information for target classification.
- The way of movement strategy can influence the observation efficiency.
- The 3D free movement(hovering) may improve the chance to find classification cues from individually incomplete and distorted echoes.

8 Conclusions

This paper has presented two methods for natural landmark classification with Biosonar. After comparison of those two methods, a two step classification strategy for mobile robot's navigation in natural environment was discussed. Those methods can be easily be transformed to recognize other multi-facet targets with Biosonar. The research tried to take some advantage of perceived properties of bats' prey identification and landmark identification mechanisms and strategies, without the claim to be a precise model of bats echolocation. Further work will include quantitatively studying the distance compensation problem in different features, trying different movement strategy, recognizing not only the target's relative bearing to the Biosonar head but also the Biosonar head's relative orientation to the target, and utilizing more advanced computation algorithms to enhance the classification performance.

Acknowledgment

The authors would like to thank Dr. Rolf Mueller for designing the sonar head with which the experiments were performed and for substantial help at the beginning of this research. The first author would like to acknowledge the financial support by the German Academic Exchange Service (DAAD) during his PhD scholarship at the University of Tübingen.

References

1. Billur Barshan. Radius of curvature estimation and localization of targets using multiple sonar sensors. *J. Acoust. Soc. Am.*, page 105(4), April 1999.
2. Carl W Baum. A sequential procedure for multihypothesis testing. In *Transactions on Information Theory*, pages 1994–2007, Nov 1994.
3. Ratner D. and McKerrow. Landmark recognition with ctfm ultrasonic sensing. In *Proceedings ACRA2001*, pages 104–110, Nice, France, 2001.
4. Riquimaroux H Gaioni SJ and Suga N. Biosonar behavior of mustached bats swung on a pendulum prior to cortical ablation. *J Neurophysiol*, 64(6):1801–17, 1990.
5. B. R. Glasberg and B. C. J Moore. Derivation of auditory filter shapes from notched-noise data. *ar. Res.*, 47:103–138, 1990.
6. A. Heale and L. Kleeman. Fast target classification using sonar. In *IEEE/RSJ International Conference on Intelligent Robots and Systems*, pages 1446–1451, Oct. 2001.
7. Huopaniemi J and Savioja L. Modeling of reflections and air absorption in acoustical spaces: a digital filter design approach. In *IEEE Workshop on Applications of Signal Processing to Audio and Acoustics*, pages 19–22, Oct 1997.
8. Probert P. Kao G. and Lee D. Object recognition with fm sonar: An assistive device for blind and visually-impaired people. In *AAAI Fall Symposium on "Developing Assistive Technology for People with Disabilities*, pages 9–11, November 1996.
9. Phillip John Mckrrow and Neil Lindsay Harper. Recognizing leafy plants with in-air sonar. *Sensor review*, 19:202–206, 1999.
10. Rolf Müller. A computational theory for the classification of natural biosonar targets based on a spike code. *Comput Neural Syst*, 14:595–612, 2003.
11. R. Muller and R. Kuc. Foliage echoes: A probe into the ecological acoustics of bat echolocation. *J. Acoust. Soc. Am.*, 108:836–45, Aug 2000.
12. Müller R. Carmena J. Hallam Peremans, H. A biomimetic platform to study perception in cf-bats. In *Sensor Fusion and Decentralized Control in Robotics Systems III*, volume 4196, Nov. 2000.

13. Hanke S Schmidt S and Pillat J. The role of echolocation in the hunting of terrestrial prey - new evidence for an underestimated strategy in the gleaning bat. *J Comp Physiol*, 186:975–988, 2000.
14. Lavender W.A. B.A. Simmons, J.A. Target structure and echo spectral discrimination by echolocating bats. *Science*, 186:1130–1132, 1974.
15. Irino T. and Patterson R.D. A time-domain, level-dependent auditory filter: The gammachirp. *J. Acoust. Soc. Am.*, 101:412–419, 1997.
16. D von Helversen. Object recogition by echolocation: a nectar-feeding bat exploiting the flowers of a rain forest vine. *J Comp Physiol*, 189:327–336, 2003.